Available online at www.sciencedirect.com
ScienceDirect
Carbohydrate Research 342 (2007) 1291–1304
Carbohydrate RESEARCH

DFT studies of the role of C-2–O-2 bond rotation in neighboring-group glycosylation reactions

Dennis M. Whitfield[a,*] and Tomoo Nukada[b]

[a]*Institute for Biological Sciences, NRC Canada, 100 Sussex Drive, Ottawa, ON, Canada K1A 0R6*
[b]*Department of Fermentation Science, Faculty of Applied Bioscience, Tokyo University of Agriculture, Sakuragaoka, 1-1 Setagayaku, Tokyo 156-8502, Japan*

Received 20 December 2006; received in revised form 26 March 2007; accepted 30 March 2007
Available online 14 April 2007

Abstract—Although the synthetic utility of the 1,2-trans relationship of the products of neighboring group participation is well established, it is still common to find glycosylation reactions where the stereochemical purity of the products is not 100%. As part of an ongoing series of density functional theory (DFT) studies of the factors that affect glycosylation reactions which are aimed at allowing synthetic chemists to achieve such selectivities, the structures of four oxacarbenium ions and eight methanol complexes of these ions were optimized for the prototypical ions 2-*O*-acetyl-3,4,6-tri-*O*-methyl-D-gluco- (**1**) and mannopyranos-1-yl (**2**). These studies corroborate the two-conformer hypothesis and further demonstrate that glycopyranosyl oxacarbenium ions exhibit facial selectivity that depends on, besides the inherent steric and Van der Waals effects, the conformational effect associated with the change from sp^2 to sp^3 hybridization at C-1 during nucleophilic attack and H-bonding between the incoming nucleophile and the electronegative atoms of the electrophile. Further studies based on systematic C-2–O-2 bond rotations found TSs that connect the monocyclic ions with the bicyclic ions associated with neighboring-group participation. It was also possible to find two TSs that connect nucleophilic attack at C-1 with C-2–O-2 bond rotation ultimately leading to 1,2-trans O-glycosides, that is, the probable TS that determines the stereochemistry of neighboring-group participation. Both of these TSs exhibit intramolecular H-bonding, which is considered the first step in proton transfer. It is further hypothesized that this coupling of proton transfer and nucleophilic attack is integral to glycosylation. It is further hypothesized that in many cases analogous intermolecular H-bonding is also favorable with the most likely acceptor the anion that is ion-paired to the oxacarbenium ion. These general features are found for both **1** and **2**, but characteristic features of each isomer are found that provide further insights into the origins of stereoselectivity.

Keywords: Glycosylation; Neighboring group participation; Transition states; DFT

1. Introduction

The increasing demand for biologically active oligosaccharides hastens the efforts to improve the efficiency of glycosylation chemistry. In particular, if polymer-supported and related technologies are ever to be used to produce oligosaccharides on industrial scale, then glycosylation reactions require at least 99% yields of the desired stereoisomer. Thus, there is a need to reduce side reactions and optimize stereoselectivity.[1] Since the transition state (TS) in most of the commonly used glycosylation chemistries is an oxacarbenium ion, one of the tactics that can be pursued is detailed studies of such ions.[2] Since such species have short lifetimes and are therefore difficult to study experimentally, one of the strategies is to use modern electronic structure calculations to estimate their properties such as probable modes of formation, probable sites of reactivity, facial selectivity, and mechanisms of interconversions.[3] To this end our group has been using density functional theory (DFT) quantum mechanical (QM) methods to study some of these aspects of prototypical glycopyranosyl oxacarbenium ions.[4] This study presents our

* Corresponding author. Tel.: +1 613 993 5265; fax: +1 613 952 9092; e-mail addresses: dennis.whitfield@nrc.ca; dennis.whitfield@nrc-cnrc.gc.ca

0008-6215/$ - see front matter © 2007 Elsevier Ltd. All rights reserved.
doi:10.1016/j.carres.2007.03.030

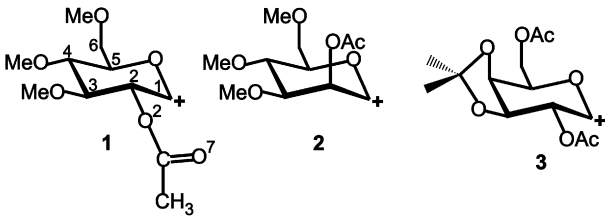

Scheme 1. Chemical structures of ions considered in this study.

current thoughts on the formation of five-membered dioxolenium ions from 2-*O*-acetyl-3,4,6-tri-*O*-methyl-D-gluco- (**1**) and mannopyranos-1-yl (**2**) oxacarbenium ions and their reactivity toward the model nucleophile methanol[5] (see Scheme 1 for structures considered). We present data on the importance of rotation about the C-2–O-2 bond and the pyranose ring conformations in these species and processes.

Since the pioneering work of Winstein, Isbell, and many others,[6] it has been recognized that groups capable of neighboring-group participation such as esters provide a powerful stereodirecting method leading to 1,2-trans glycosides often exclusively and often in high yields, although rarely as high as 99%. The original formulation of this participatory mechanism focused on the kinetic aspect as exemplified by the greater reactivity of 1,2-di-*O*-acetyl derivatives of β-D-glucopyranose as compared to their α anomers.[7] In recent years, where much more reactive leaving groups than acetate are typically used in glycosylation reactions, the thermodynamic aspects of bicyclic dioxolenium ion formation leading to 1,2-*trans* glycosides has gained more importance. However, in some cases stereoselectivity is not complete, some amount—and even occasionally predominantly—of the 1,2-*cis* glycosides are formed. The most frequent rationalization is that the cis-glycosylation reaction proceeds through the monocyclic oxacarbenium ion.[8] Thus, it is of some interest to determine the factors, and if possible the transition states, associated with the interconversion of such monocyclic and bicyclic ions. Our previous static DFT studies of the relatively rigid 2,6-di-*O*-acetyl-3,4-*O*-isopropylidene-D-galactopyranosyl oxacarbenium ion (**3**) found that both the oxacarbenium ions (**B0** and **B1**) and the dioxolenium ions (**C0** and **C1**) have at least two stable conformations that differ by ring inversion. The **C0** and **C1** ions were found to be considerably more stable then the **B0** and **B1** ions, suggesting their importance in glycosylation reactions.[5b] Further constrained ab initio molecular dynamics (AIMD) studies found compelling evidence for an interconversion pathway that involved initial ring inversion followed by almost barrierless C-2–O-2 bond rotation with an overall barrier of 34 kJ mol^{-1}.[9] Determining whether or not this inversion–rotation pathway is normal or a special case for **3** is one of the questions addressed in this work. Note that glycosyl donors related to **3** were found experimentally to exhibit a marked propensity to give an acyltransfer side reaction.[5c] Examination of a possible TS in a proton transfer to O-2 triggered pathway for **3** led to the synthetic development of 2,6-dimethylbenzoyl and 2,6-dimethoxybenzoyl protecting groups that greatly minimize this side reaction.[5e]

The **B0** and **B1** species have a lowest unoccupied molecular orbital (LUMO) mostly positioned between O-5 and C-1, suggesting that nucleophilic attack should occur at C-1 as usually observed.[10] Nucleophilic attack on the β face of such ions leads to **F0** and **F1** ions whereas α face attack leads to **G0** and **G1** ions. The **C0** and **C1** ions have a LUMO with a high degree of p-orbital character centered on C-7, the former carbonyl carbon in the dioxolenium ion.[5b] This suggests that nucleophilic attack should first occur at C-7, followed by some process that leads to attack at C-1.[11] We name the associated methanol complexes as **D0** and **D1** and **E0** and **E1**. Thus, as shown in Scheme 2 for **1** and Scheme 3 for **2**, at least 12 species need to be considered. Species **A** are the corresponding glycosyl donors and are not considered in detail in this work. Nonspecific solvation is considered using a continuum dielectric method parameterized to CH_2Cl_2, a solvent often used in glycosylation reactions. Neither direct solvent participation or ion pairing is considered in our current QM methods. Since there is considerable evidence that both these factors are important,[12] at least in some cases, this deficiency remains for future work. Nonetheless, it is hoped that determination of the 12 minimum-energy species **B0** to **G1** for **1** and **2**, as well as some of their interconversion pathways, will assist synthetic chemists to develop efficient glycosylation methodologies.

2. Methods

The DFT calculations were carried out with the Amsterdam density functional (ADF) program system, ADF2005.[13] The atomic orbitals were described as an uncontracted triple-ζ Slater function basis set with a single-ζ polarization function on all atoms that were taken from the ADF library (TPZ). The 1s electrons on carbon and oxygen were assigned to the core and treated by the frozen-core approximation. A set of s, p, d, f, and g Slater functions centered on all nuclei were used to fit the electron density and to evaluate the Coulomb and exchange potentials accurately in each SCF cycle. The local part of the V_{xc} potential (LDA) was described using the VWN parametrization,[14] in combination with the gradient-corrected (CGA) Becke's functional[15] for the exchange and Perdew's function for correlation (BP86).[16] The CGA approach was applied self-consistently in geometry optimizations. Second derivatives were evaluated numerically by a two-point formula.

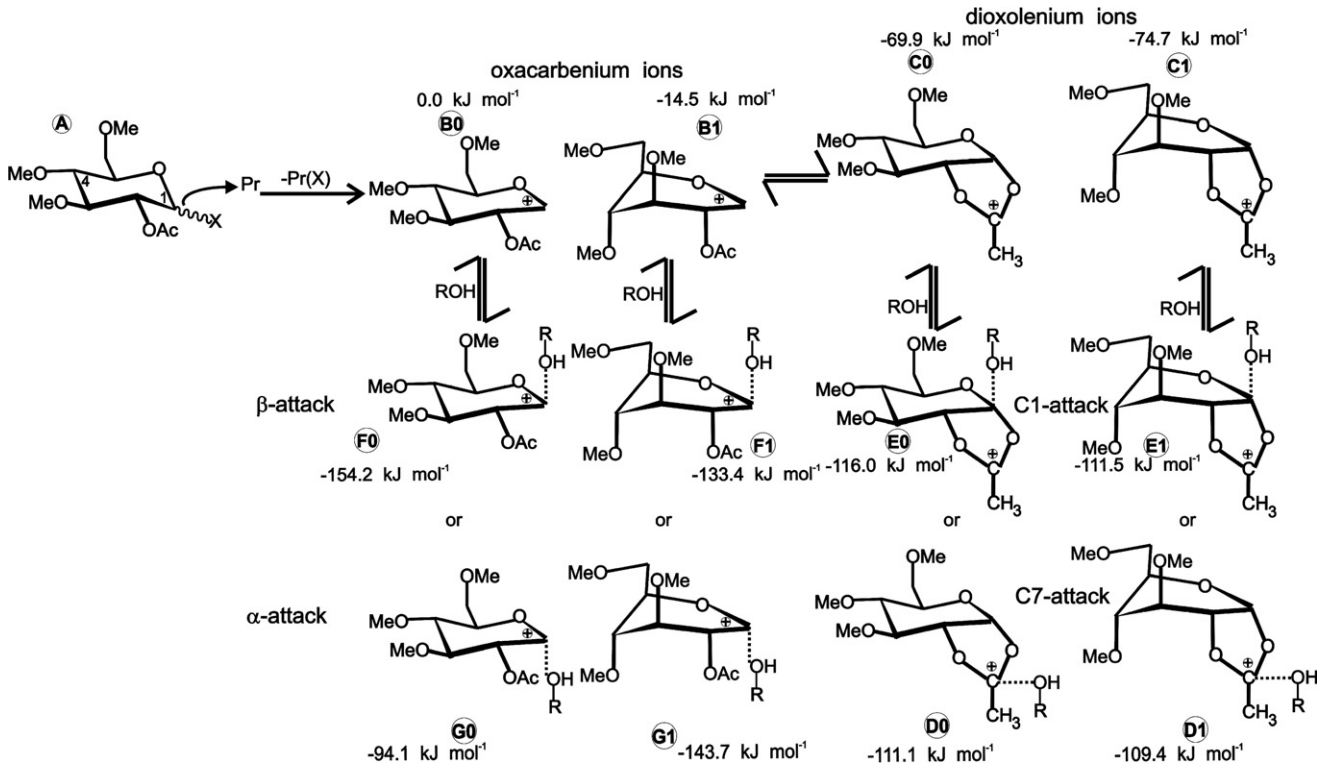

Scheme 2. Species **A** to **G1** for gluco-configured **1**. The numbers are the relative energies in kJ mol^{-1} (see Section 2). The ring structures are drawn to emphasize the ring inversion which distinguishes **B0**–**G0** from **B1**–**G1** and do not represent the actual conformations.

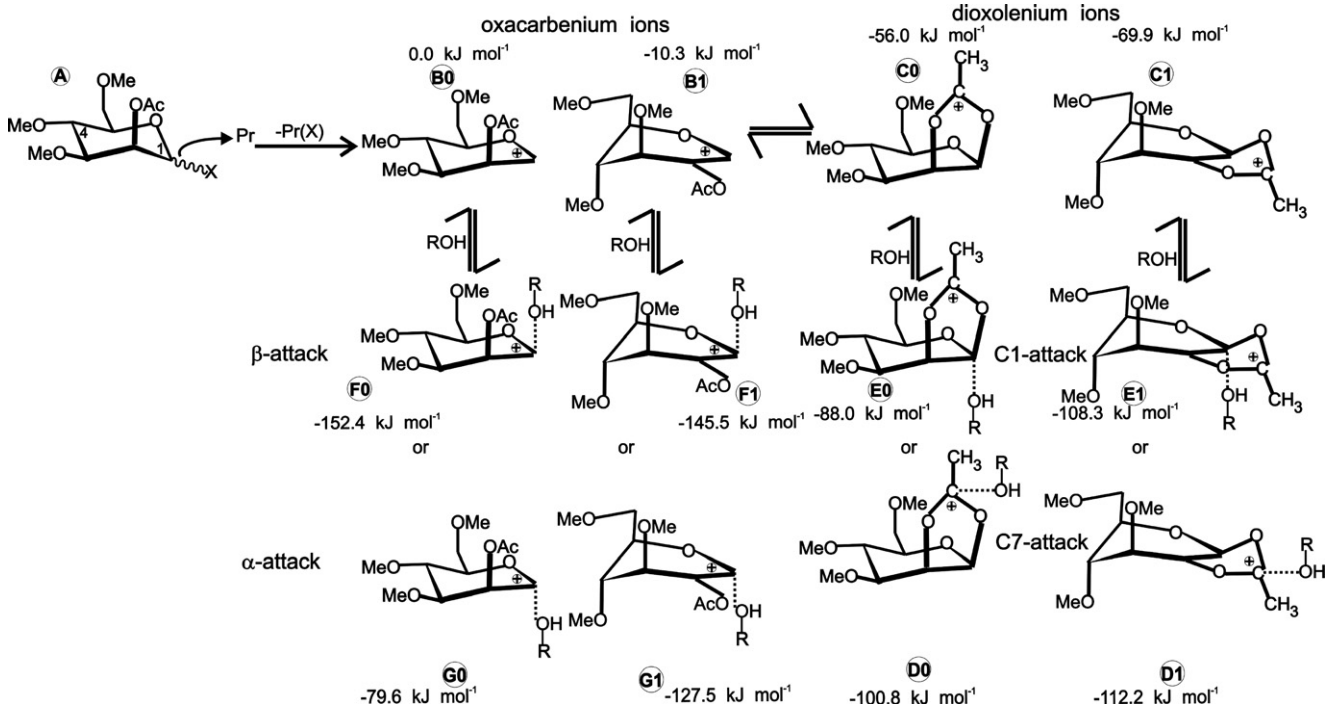

Scheme 3. Species **A** to **G1** for manno configured **2**. The numbers are the relative energies in kJ mol^{-1} (see Section 2). The ring structures are drawn to emphasize the ring inversion which distinguishes **B0**–**G0** from **B1**–**G1** and do not represent the actual conformations.

The solvation parameters were dielectric constant $\varepsilon = 9.03$, ball radius = 2.4 Å, with atomic radii of C = 1.7, O = 1.4 and H = 1.2 Å and were taken from the default ADF values.

Initial **B0** and **B1** structures were generated from the optimized **B0** or **B1** conformations of the tetra-*O*-methyl analogues[4b] and by starting from idealized $^4H_3$ or $^3H_4$ conformations,[17] followed by optimization with an integration accuracy of 6.5 and using internal coordinates. Both starting conformations optimized to similar structures. **C0** and **C1** conformations were generated from the optimized **B0** and **B1** conformations by C-2–O-2 bond rotations of ±120°, followed by optimization as below. Subsequently **D0** to **G1** methanol complexes were formed by adding methanol to the appropriate face of the molecule and optimizing as below. After initial optimization it was often found, as indicated by frequency calculations, that one or more methyl groups were not in a minimum conformation. The appropriate methyl group was then rotated as indicated by the coefficients of the imaginary frequency and the structure reoptimized with a higher integration accuracy of 8.5. In some cases the resulting structures were still not a minimum. In this case intrinsic reaction coordinate (IRC) calculations were used following the imaginary frequency going both forward and backward. Then the lowest of the forward or backward pathways energy, conformation was reoptimized and checked as a minimum. In a few cases the process had to be repeated several times before a minimum was found. Then the C-5–O-6 dihedral angle was optimized using a linear transit (LT) procedure by rotating this internal coordinate in twelve 30° increments. If a lower energy conformer was found, it was reoptimized. In this way all reported minima have optimized side-chain conformers.

To investigate **B0** to **C0**, **B1** to **C1**, **E0** to **F0** (or **G0** for **2**), and **E1** to **F1** (or **G1** for **2**) interconversions LT procedures, rotating the C-2–O-2 dihedral angle in thirty-six 10° increments in either direction were done. Both rotation directions were studied to insure reproducibility. Apparent TS's (maxima) from the resulting energy versus dihedral angle plots were then tested by frequency calculations. Then, the lowest imaginary frequency was used in a transition-state optimization. The resulting conformation was then checked by frequency calculation to have one imaginary frequency. The coefficients of this frequency were then checked to insure that they correspond to the atoms expected to be involved in the TS, typically CH-2, C-2, O-2, C(=O), (C=)O, (C=)CH_3 and C-1, CH-1. If methanol was in the study, its atoms were also found.

3. Results and discussion

All 12 species for each of gluco-configured **1** and manno configured **2** were fully optimized (see Section 2 for details). Ball-and-stick representations are shown in Figure 1a–n for **1** and in Figure 2a–l for **2**. For **1** two additional species **F0′** and **F1′** were also found. These species are included, even though they are higher in energy than

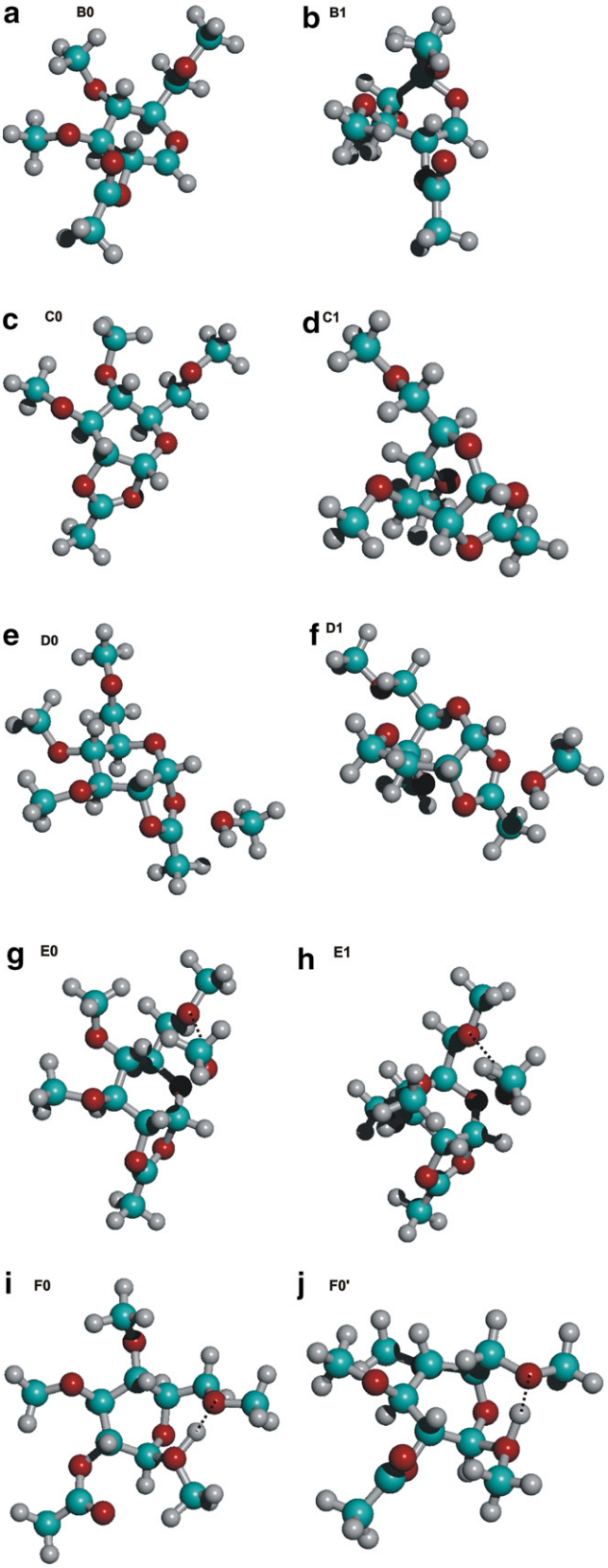

Figure 1. Ball-and-stick representations of the optimized conformations of **1** (a) **B0**, (b) **B1**, (c) **C0**, (d) **C1**, (e) **D0**, (f) **D1**, (g) **E0**, (h) **E1**, (i) **F0**, (j) **F0′**, (k) **F1**, (l) **F1′**, (m) **G0**, (n) **G1**.

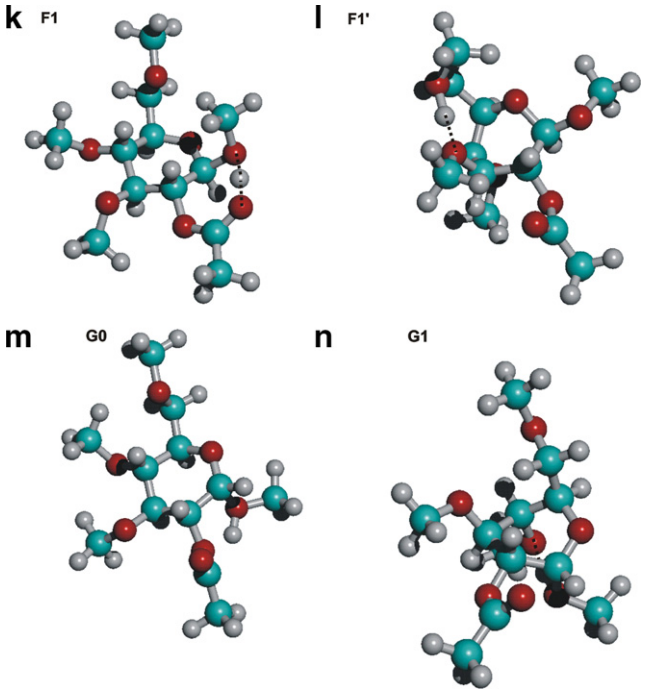

Figure 1 (*continued*)

F0 or **F1** because they represent significantly different structures. Species **F1′** has the hydroxylic proton transferred to O-6 and is a plausible intermediate on the way to glycosides in the absence of external bases. Similarly **F0′** has the hydroxylic proton H-bonded to the carbonyl oxygen attached to O-2 (O-7), and although not the minimum for this minimally protected prototype, it is a plausible species for donors with different protecting groups. Note that both **F0** and **F1** for **1** and **2** have strong H-bonds to O-6, and therefore the protecting group at O-6 is expected to markedly influence the stability of the **F0** and **F1** species.

The relative energies and selected bond lengths, bond angles, and torsion angles of these 26 species are compiled in Table 1. The ring conformations of all stationary points are tabulated in Table 2 using the canonical vector representation. A complete description of the canonical vector representation is provided in the references.[17,5f] In short, all the conformations of six-membered rings can be conveniently expressed as combinations of the three coordinates, and in accord with standard IUPAC nomenclature these are termed chair, skew boat, and boat conformations. This allows the conformations to be plotted on a three-dimensional sphere, thus providing an easy graphical representation. On this sphere the poles correspond to the two chair conformations, and the boat and skew boats lie along the equator. Two sets of half chair and envelope conformations lie halfway between the equator and either pole (see Fig. 3). As an illustrative example the **B0** conformation of **1** has the following three principal $^{4}C_{1}$ 0.513 $^{2,5}B$

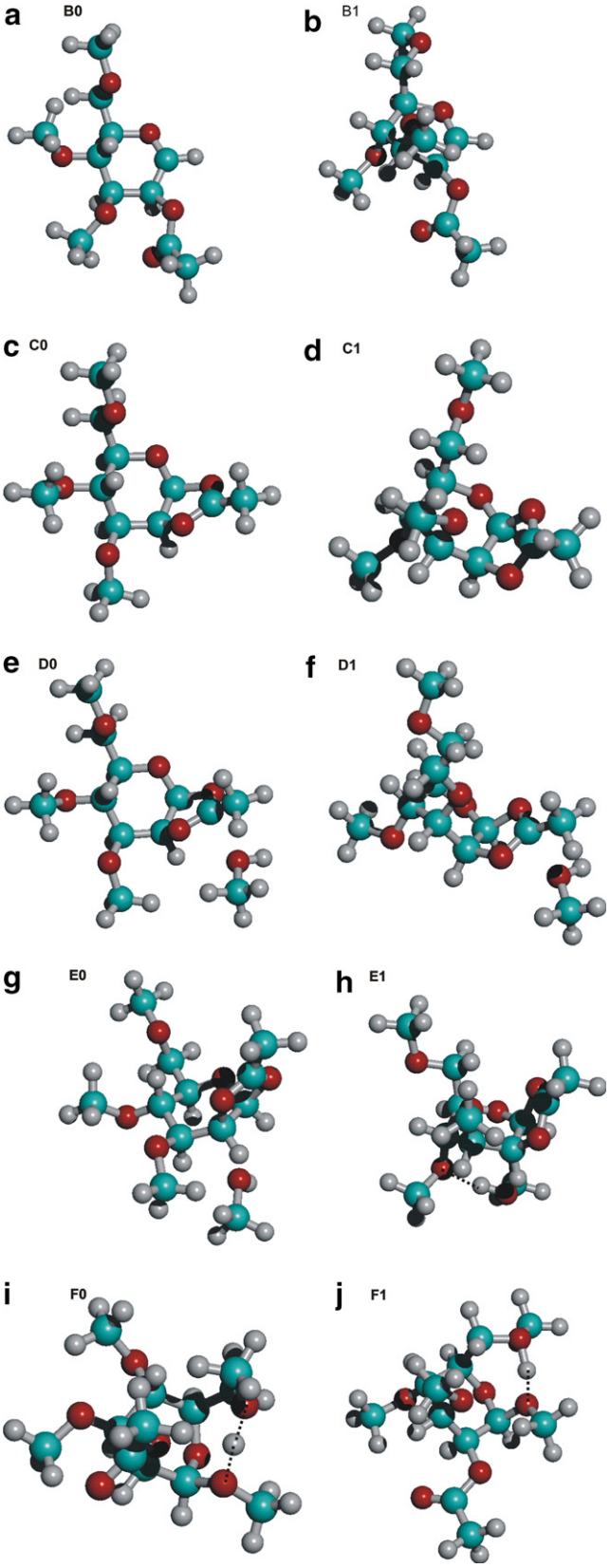

Figure 2. Ball-and-stick representations of the optimized conformations of **2** (a) **B0**, (b) **B1**, (c) **C0**, (d) **C1**, (e) **D0**, (f) **D1**, (g) **E0**, (h) **E1**, (i) **F0**, (j) **F1**, (k) **G0**, (l) **G1**.

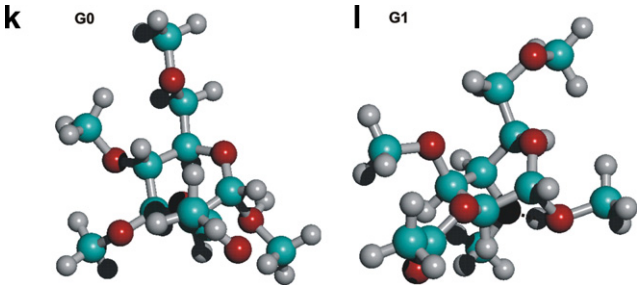

Figure 2 (*continued*)

0.098 $^{1}S_{3}$ 0.477 vectors showing that this conformation is nearly exactly half a chair and half a skew boat with a small boat component. Thus, it is nearly a perfect half chair, $^{4}H_{3}$ 0.953. The corresponding ring torsion angles are compiled in Table 3 where τ_1 = C-1–C-2–C-3–C-4, τ_2 = C-2–C-3–C-4–C-5, etc.

For both **1** and **2** two sets of species **B0**–**G0** and **B1** to **G1** that conform to the two conformer hypotheses were found (Fig. 3a and b).[4b] **B0**–**G0** for **1** and all but axial O-2 in **2** keep all substituents pseudoequatorial, whereas species **B1** to **G1** are ring inverted. Importantly and as previously found for other gluco-configured ions, **B1**, **F1** and **G1** species are found in a $^{5}S_{1}$ conformation that allows O-2 to be pseudoequatorial, whereas all other substituents are pseudoaxial (Fig. 1b, k, and n).[10] For the **2** **B1** to **G1** species, this allows O-2 to be pseudoequatorial and all other substituents pseudoaxial (Fig. 2b, d, f, h, and l). These new results strongly corroborate our finding of a marked preference for the electronegative substituent at C-2 to be pseudoequatorial in glycopyranosyl oxacarbenium ions. This result has important implications for the reactivity of such ions including the question of the design of TS inhibitors for glycosyl processing enzymes (GPE) that are believed to have oxacarbenium ion-like TSs.[18]

As above for **1**, the **B0** ring conformation is almost 100% $^{4}H_{3}$ which is long expected to be the preferred conformation for gluco-configured glycopyranosyl oxacarbenium ions. The tetramethyl analogue of **2** was found to have a $^{4}H_{3}$ conformation with O-2 axial, but for **2** a conformation distant from any of the 38 IUPAC conformations which is best characterized as $^{4}H_{5}$ 0.686 was found. Examination of Figure 2a shows that this also allows O-2 to be close to pseudoequatorial again showing the importance of this effect. The origin of this effect is not clear, but is thought to be related to favorable interactions between the lone pairs on O-2 and the double bond like LUMO between C-1 and O-5. Since such effects are challenging to accurately calculate,[19] it is anticipated that as software and hardware improvements become available a more detailed analysis of this effect may be possible. At the current DFT level (see Section 2), the **B1** species are >10 kJ mol^{-1} more stable than the **B0** species, suggesting that if these species are sufficiently long lived to equilibrate, these will be the dominant conformations.[20] Furthermore, if such species subsequently react with nucleophiles such as methanol, then species **F1** and **G1** are likely intermediates whose stability could in part control the stereoselectivity of the glycosylation reaction.

Ring closure to form the **C0** and **C1** dioxolenium ions involves for **1** a net movement of O-7 from the β face to the α face or for **2** from the α face to the β face (see Fig. 1c, d and 2c, d). This requires large changes in the CH-2-C-2–O-2-O-7 torsion angle, see Table 1. As could be expected from the delocalization of charge into the five-membered ring the O-5–C-1 bond lengthens by about 0.06 Å on going from the **B** to the **C** species in all cases. What is less easily deduced or explained is that C-1–C-2 increases by about 0.08 Å on going from the **B** to the **C** species whereas C-5–O-5 decreases by about 0.03 Å. The ring conformation for **C0** of **1** is a chair ($^{4}C_{1}$ 0.747), but the large skew boat coefficient ($^{1}S_{5}$ 0.287) shows that the conformation is close to $^{4}H_{5}$ and can be seen as a pseudorotation to allow C-1–C-2 to approach planarity rather than O-5–C-1. A similar trend is observed for **C1** of **1** where a pseudorotation from **B1** $^{5}S_{1}$ to near $^{3}S_{1}$ is all that is necessary. The β-face ring closure to form **2** **C0** or **C1** in both case leads to chair conformations.

The ω_H (CH-5-C-5–C-6-O-6) conformation varies among all species, and in most cases takes values near the expected *gg* ($\omega_H = 180°$) and *gt* ($\omega_H = -60°$) rotamers for all species. However, for **1** **C1**, **D1**, and **G1**, as well as for **2** **D1** and **E1**, the unusual *tg* ($\omega_H = 60°$) conformation was found. No obvious correlation between energetic stability and ω_H conformation is observed except for the cases where substituents attached to C-6 are involved in H-bonding interactions. The geometric characteristics of all intramolecular H-bonded species are compiled in Table 4.

Conventional descriptions of glycopyranosyl oxacarbenium ions consider that τ_5 should be near 0° as the O-5–C-1 bond should have considerable double-bond character and C-1 considerable sp^2 character.[21] However, only the isolated **B0** and **B1** ions exhibit this feature. All other ions that have additional bonding to C-1 show considerable deviation from planarity, that is, τ_5 has markedly nonzero values, see Table 3. This is true for both **1** and **2**, but there are significant differences between them notably for the neighboring-group ions **C0** to **E1**. For such gluco-configured ions, τ_6 has small values showing that the C-1–C-2 bond approaches planarity to allow for dioxolenium ion formation, whereas this does not occur for manno-configured ions that form dioxolenium ions with chair conformations only slightly distorted toward boat or skew boat conformations (see Tables 2 and 3). This result also has implications for GPE TS inhibitor design, as considerable synthetic effort has been directed at mimicking ions with planar τ_5.

Table 1. Selected geometric variables and relative energies of oxacarbenium ions **B0**, **B1** to **G1** for **1** and **2**

Compound	C-5–O-5 (Å)	O-5–C-1 (Å)	C-1–C-2 (Å)	C-1–OCH_3 (Å)	CH-2-C-2–O-2-O-7 (°)	CH-5-C-5–C-6-O-6 (°)	ΔE[a] (kJ mol^{-1})
1 B0	1.473	1.261	1.436	—	12.9	−179	0
1 B1	1.475	1.268	1.433	—	1.5	−157.3	−14.5
1 C0	1.444	1.321	1.511	—	−140.8	173.9	−69.9
1 C1	1.44	1.334	1.526	—	−133.2	54.2	−74.7
1 D0	1.438	1.331	1.517	2.1942	−134.5	174.2	−111.1
1 D1	1.438	1.335	1.524	2.5952	−126.3	52.5	−109.4
1 E0	1.442	1.321	1.509	2.766	−139.9	175.1	−116
1 E1	1.439	1.332	1.524	2.689	−129.8	−171.4	−111.5
1 F0	1.433	1.372	1.526	1.468	−48.3	177.6	**−154.2**
1 F0′	1.432	1.355	1.52	1.469	−52.8	177.8	−134.7
1 F1	1.431	1.367	1.513	1.474	6.7	−85.2	−143.7
1 F1′	1.415	1.427	1.507	1.363	30.8	−175.9	−133.4
1 G0	1.452	1.323	1.508	1.571	−4.4	173.1	−94.1
1 G1	1.441	1.364	1.507	1.483	−37.1	56.2	−140
2 B0	1.481	1.261	1.439	—	−40.4	177.5	0
2 B1	1.47	1.264	1.432	—	−23.1	−51.4	−10.3
2 C0	1.433	1.366	1.511	—	94.2	171.8	−56
2 C1	1.449	1.32	1.509	—	149.1	−39.1	−69.9
2 D0	1.429	1.373	1.51	2.18	85.2	170.2	−100.8
2 D1	1.437	1.334	1.514	2.261	142.9	64.2	−112.2
2 E0	1.433	1.367	1.513	2.86	96	170.7	−88
2 E1	1.44	1.329	1.511	2.924	146	60.4	−108.2
2 F0	1.433	1.377	1.523	1.456	−14.7	−174.8	**−152.4**
2 F1	1.437	1.378	1.509	1.454	−38.5	−98.1	−145.3
2 G0	1.455	1.324	1.507	1.595	35.4	172.3	−79.6
2 G1	1.439	1.363	1.518	1.483	−39.1	−49.3	−127.5

[a] Relative energies including ZPE at the TPZ DFT level, including isolated methanol for the **B** and **C** species. For each of **1 B0** and **2 B0** set to 0.0 kJ mol^{-1}, absolute energies for **1 B0** are −7.64368506 a.u. and for **2 B0** −7.64215867 a.u. With MeOH at this level the absolute energy is −1.11661603 a.u (1 a.u. = 2625.4985 kJ).

Many GPE TSs likely have some appreciable degree of interaction with either the incoming nucleophile or the departing leaving group and therefore have a nonplanar τ_5 which should be considered when designing mimics.[22]

For all dioxolenium ions of both **1** and **2**, methanol complexation causes only small pyranosyl ring conformational changes from the parent **C0** or **C1** conformations to any of **D0**, **D1**, **E0** or **E1** complexes. In all these cases the CH_3O–C-1 bond length is greater than 2 Å, suggesting a strong ion–dipole interaction. In marked contrast, methanol complexation with **B0** and **B1** ions leads to species with CH_3O–C-1 bond lengths near 1.5 Å, which can be considered hydronium ions. The C-5–O-5, O-5–C-1, and C-1–C-2 bond lengths all change comparably to the **B** to **C** case, suggesting charge delocalization in this case onto the incoming nucleophile. These charge effects may also explain the nonplanarity of τ_5 discussed above, which are further coupled to ring conformational changes that can be either favorable or unfavorable. For example, α attack on **B0** ions leads toward chair conformations and is favorable. Whereas β attack on the same **B0** ions leads to unfavorable boat (**2 F0**) or skew boat (**1 F0**) conformations. Viewed on the three-dimensional sphere α attack corresponds to movement toward the poles, whereas β attack is toward the equator. For **2 B1** just the opposite happens with α attack (**G1**) leading to a skew boat and β attack (**F1**) a chair. Again showing a distinct difference between manno and gluco configurations, α attack (**G1**) or β attack (**F1**) on **1 B1** leads to only small pyranosyl ring conformational changes. These last results again show the stability of the $^5S_1$ conformation of **1** that allows O-2 to be pseudoequatorial and hence lie close to the plane of the O-5–C-1 double bond.[10]

One clear trend is that β glycosylation is favored by intramolecular H-bonding to O-6 in the **F** species. This is a factor that synthetic chemists can control by choosing O-6 protecting groups. That is, small electron-donating protecting groups should favor β glycosylation, whereas α glycosylation should be favored by large electron-withdrawing groups. Attempts to promote α glycosylation through the use of bulky protecting groups is well known[23] and is known to require very large groups for high selectivity. It has also been shown that α/β selectivities follow a Hammett relationship in the directions suggested above, providing further evidence that, at least in some cases, α/β selectivities can be controlled by favoring or disfavoring H-bonding.[24]

As noted by another author,[25] it is difficult to reconcile these thermodynamically stable species (**B0** to **G1**) with the fact that in most modern glycosylation reactions stereoselectivity is kinetically controlled. Notably the conventional model of neighboring-group participation would have **E**-like complexes as the closest to the TS. If the energy barrier to neutral glycosides was the same for every **E** species, and the relevant **E** species

Table 2. Canonical vector coefficients for the pyran rings of oxacarbenium ions **B0**, **B1** to **G1** for **1** and **2**

Compound	Chair	Boat	Skew boat	Intermediate	1st	2nd
1 B0	$^{4}C_1$ 0.513	$^{2,5}B$ 0.098	$^{1}S_3$ 0.477	$^{4}\boldsymbol{H_3}$ **0.953**	$^{2,5}B$ 0.098	$^{4}C_1$ 0.037
1 B1	$^{1}C_4$ 0.256	$^{0,3}B$ 0.044	$^{5}\boldsymbol{S_1}$ **0.847**	$^{5}S_1$ 0.847	$^{1}C_4$ 0.256	$^{0,3}B$ 0.044
1 C0	$^{4}\boldsymbol{C_1}$ **0.747**	$^{0,3}B$ 0.004	$^{1}S_5$ 0.287	$^{4}C_1$ 0.747	$^{0,3}B$ 0.004	$^{1}S_5$ 0.287
1 C1	$^{1}C_4$ 0.116	$B_{2,5}$ 0.090	$^{3}\boldsymbol{S_1}$ **0.883**	$^{3}S_1$ 0.883	E_2 0.181	$^{1}C_4$ 0.026
1 D0	$^{4}\boldsymbol{C_1}$ **0.753**	$^{0,3}B$ 0.039	$^{1}S_5$ 0.291	$^{4}C_1$ 0.753	$^{1}S_5$ 0.291	$^{0,3}B$ 0.039
1 D1	$^{1}C_4$ 0.103	$B_{2,5}$ 0.120	$^{3}\boldsymbol{S_1}$ **0.869**	$^{3}S_1$ 0.869	E_2 0.205	$B_{2,5}$ 0.886
1 E0	$^{4}\boldsymbol{C_1}$ **0.659**	$B_{2,5}$ 0.064	$^{1}S_3$ 0.284	$^{4}C_1$ 0.659	$^{1}S_3$ 0.284	$B_{2,5}$ 0.064
1 E1	$^{1}C_4$ 0.165	$^{2,5}B$ 0.054	$^{3}\boldsymbol{S_1}$ **0.712**	$^{1}C_4$ 0.165	$^{3}S_1$ 0.712	$^{2,5}B$ 0.054
1 F0	$^{4}C_1$ 0.124	$^{2,5}B$ 0.096	$^{1}\boldsymbol{S_3}$ **0.986**	$^{1}S_3$ 0.986	^{2}E 0.193	$^{4}C_1$ 0.028
1 F0′	$^{4}\boldsymbol{C_1}$ **0.654**	$B_{0,3}$ 0.324	$^{1}S_5$ 0.077	$^{4}C_1$ 0.654	$B_{0,3}$ 0.324	$^{1}S_5$ 0.077
1 F1	$^{4}C_1$ 0.040	$^{0,3}B$ 0.144	$^{5}\boldsymbol{S_1}$ **0.936**	$^{5}S_1$ 0.936	$^{0,3}B$ 0.144	$^{4}C_1$ 0.040
1 F1′	$^{1}C_4$ 0.234	$B_{1,4}$ 0.196	$^{2}\boldsymbol{S_0}$ **0.859**	$^{2}S_0$ 0.859	E_4 0.391	$^{1}C_4$ 0.138
1 G0	$^{4}\boldsymbol{C_1}$ **0.808**	$^{1,4}B$ 0.136	$^{0}S_2$ 0.030	$^{4}C_1$ 0.808	$^{1,4}B$ 0.136	$^{0}S_2$ 0.030
1 G1	$^{4}C_1$ 0.209	$B_{0,3}$ 0.214	$^{5}\boldsymbol{S_1}$ **0.810**	$^{5}S_1$ 0.810	E_3 0.418	$B_{0,3}$ 0.814
2 B0	$^{4}C_1$ 0.343	$B_{0,3}$ 0.144	$^{1}S_5$ 0.668	$^{4}\boldsymbol{H_5}$ **0.686**	$^{1}S_5$ 0.325	$B_{0,3}$ 0.144
2 B1	$^{1}C_4$ 0.545	$^{0,3}B$ 0.487	$^{5}S_1$ 0.041	$^{3}\boldsymbol{E}$ **0.975**	$^{5}H_4$ 0.081	$^{1}C_4$ 0.018
2 C0	$^{4}\boldsymbol{C_1}$ **0.817**	$B_{2,5}$ 0.167	$^{1}S_3$ 0.036	$^{4}C_1$ 0.817	$B_{2,5}$ 0.167	$^{1}S_3$ 0.036
2 C1	$^{1}\boldsymbol{C_4}$ **0.753**	$^{2,5}B$ 0.046	$^{3}S_1$ 0.225	$^{1}C_4$ 0.753	$^{3}S_1$ 0.225	$^{2,5}B$ 0.046
2 D0	$^{4}\boldsymbol{C_1}$ **0.832**	$B_{2,5}$ 0.174	$^{3}S_1$ 0.002	$^{4}C_1$ 0.832	$B_{2,5}$ 0.174	$^{3}S_1$ 0.002
2 D1	$^{1}\boldsymbol{C_4}$ **0.739**	$^{2,5}B$ 0.034	$^{3}S_1$ 0.221	$^{1}C_4$ 0.739	$^{3}S_1$ 0.221	$^{2,5}B$ 0.034
2 E0	$^{4}\boldsymbol{C_1}$ **0.793**	$^{0,3}B$ 0.060	$^{1}S_5$ 0.236	$^{4}C_1$ 0.793	$^{1}S_5$ 0.236	$^{0,3}B$ 0.060
2 E1	$^{1}\boldsymbol{C_4}$ **0.716**	$B_{1,4}$ 0.145	$^{0}S_2$ 0.117	$^{1}C_4$ 0.716	$B_{1,4}$ 0.145	$^{0}S_2$ 0.117
2 F0	$^{4}C_1$ 0.113	$\boldsymbol{B_{0,3}}$ **0.864**	$^{5}S_1$ 0.100	$B_{0,3}$ 0.864	$^{2}H_1$ 0.199	$^{4}C_1$ 0.014
2 F1	$^{1}\boldsymbol{C_4}$ **0.874**	$^{1,4}B$ 0.005	$^{0}S_2$ 0.053	$^{1}C_4$ 0.874	$^{0}S_2$ 0.053	$^{1,4}B$ 0.005
2 G0	$^{4}\boldsymbol{C_1}$ **0.768**	$^{1,4}B$ 0.204	$^{2}S_0$ 0.021	$^{4}C_1$ 0.768	$^{1,4}B$ 0.204	$^{2}S_0$ 0.021
2 G1	$^{1}C_4$ 0.083	$B_{2,5}$ 0.006	$^{3}\boldsymbol{S_1}$ **1.003**	$^{3}S_1$ 1.003	$^{1}C_4$ 0.083	$B_{2,5}$ 0.006
B0–**C0** TS1 **1**	$^{4}C_1$ 0.529	$^{1,4}B$ 0.425	$^{2}S_0$ 0.042	$^{4}\boldsymbol{E}$ **0.851**	$^{4}C_1$ 0.104	$^{2}S_0$ 0.042
B0–**C0** TS2 **1**	$^{4}C_1$ 0.489	$^{1,4}B$ 0.439	$^{2}S_0$ 0.113	$^{4}\boldsymbol{E}$ **0.879**	$^{2}S_0$ 0.113	$^{4}C_1$ 0.050
B1–**C1** TS1 **1**	$^{1}C_4$ 0.240	$^{0,3}B$ 0.050	$^{5}\boldsymbol{S_1}$ **0.854**	$^{1}C_4$ 0.240	$^{0,3}B$ 0.050	$^{5}S_1$ 0.854
B1–**C1** TS1 **1**	$^{1}C_4$ 0.271	$^{0,3}B$ 0.205	$^{5}\boldsymbol{S_1}$ **0.858**	$^{5}S_1$ 0.858	^{3}E 0.411	$^{1}C_4$ 0.066
B0–**C0** TS **2**	$^{4}C_1$ 0.507	$^{2,5}B$ 0.047	$^{1}S_3$ 0.471	$^{4}\boldsymbol{H_3}$ **0.942**	^{2}E 0.072	$^{2,5}B$ 0.011
B1–**C1** TS **2**	$^{1}C_4$ 0.557	$^{0,3}B$ 0.484	$^{1}S_5$ 0.009	$^{3}\boldsymbol{E}$ **0.968**	$^{1}C_4$ 0.073	$^{1}S_5$ 0.009
E0 Gly TS **1**	$^{1}C_4$ 0.019	$B_{2,5}$ 0.224	$^{1}\boldsymbol{S_3}$ **0.882**	$^{1}C_4$ 0.019	$B_{2,5}$ 0.224	$^{1}S_3$ 0.882
E1 Gly TS **2**	$^{1}C_4$ 0.119	$B_{0,3}$ 0.130	$^{5}\boldsymbol{S_1}$ **0.783**	$^{5}S_1$ 0.783	E_0 0.28	$B_{0,3}$ 0.794

freely interconvert, then the lowest energy species would determine stereoselectivity. For **1** this would be **E0** and for **2** it would be **E1**. However, even comparing to the closest species **D**, where for **1**, **E0** is the lowest, but for **2**, **D1** is the lowest energy, more complex behavior is suggested. For example, this would suggest a tendency for 2-*O*-acyl mannopyranosyl donors to form ortho-esters rather then glycosides, that is, reaction via **D1** not **E1**. Although manno-configured orthoesters are known, this is not usually the case.[26] For all eight of these **D** and **E** species, at least three interrelated things have to happen in order to arrive at neutral species. These are that, the CH_3O–C-1 or CH_3O–C-7 bond must shorten considerably, that the hydroxylic proton must transfer, and that C-1 or C-7 must rehybridize to sp^3. That these should be of approximately the same energy seems reasonable. The exact differences are, however, difficult to estimate due to, in particular, the ambiguity over what species is the ultimate proton acceptor and what pathway the proton takes to arrive there.

The various **F** species are all intramolecularly H-bonded, and this suggests one plausible pathway type which is a proton-transfer pathway where the first step is intramolecular. In fact **1 F1′** is a possible example where the hydroxylic proton has transferred to O-6 and is H-bonded to O-4. Similarly **1 F0′** which feature a H-bond to the carbonyl oxygen suggests a variant intramolecular proton transfer pathway, which in this case involves transfer to the carbonyl oxygen of the ester protecting group.

At least one further complexity in comparing the **D** to **G** species is that the species with appreciable hydronium-ion character but no intramolecular H-bonds likely have intermolecular H-bonds since such strong acids will seek out electronegative atoms especially in weakly polar solvents like dichloromethane that are typically used in glycosylation reactions. This effect is estimated to be 28 kJ mol^{-1} based on previous work.[5d] For **1** the energetic comparisons between **B0** and **G1** fit the observed high β selectivity for 2-*O*-acyl glucopyranosyl donors considering reactions through the **E** or **F** species. However, for **2** this thermodynamic analysis fails as the observed high α selectivity, in fact typically exclusively α, for 2-*O*-acyl mannopyranosyl donors is not predicted as the **G** versus **F** or as above the **D** versus **E** selectivities are backwards, even after the

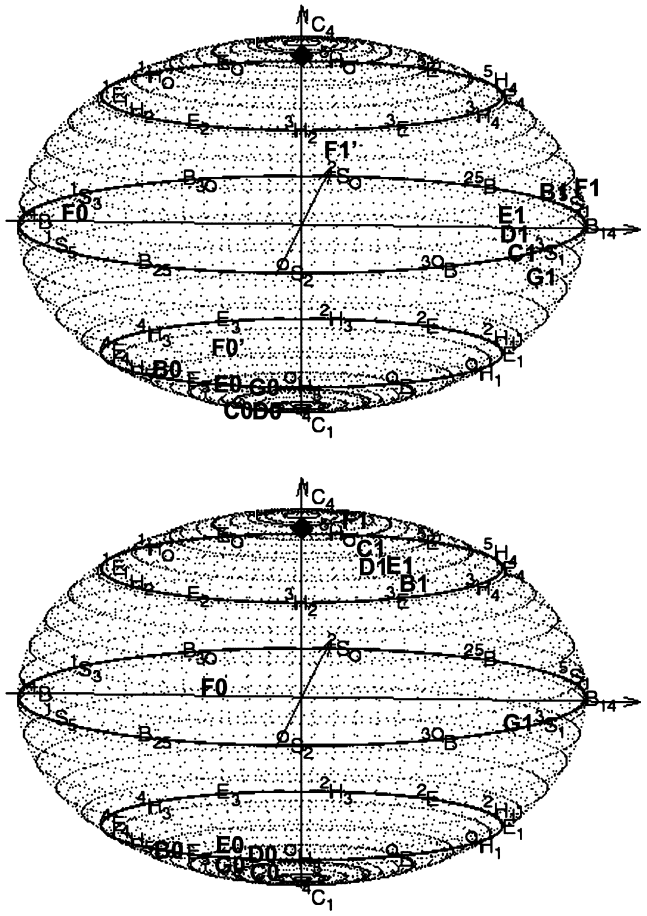

Figure 3. Spherical representations of the conformation of six-membered rings top **1** with the 14 minima placed in their approximate positions and bottom **2** with the 12 minima placed in their approximate positions. (a) Top, (b) bottom.

Table 3. Ring dihedral angles of the pyran ring of oxacarbenium ions **B0**, **B1** to **G1** for **1** and **2**

Compound	τ_1	τ_2	τ_3	τ_4	τ_5	τ_6
1 B0	−50.2	59.1	−40.2	10	−1.7	23.5
1 B1	−5.9	−42.4	66.4	−38.1	−12.1	36.8
1 C0	−36	53.2	−61.9	53.8	−36.4	27.5
1 C1	38.6	−59.1	29.1	24.9	−47.2	12.7
1 D0	−34.3	51.6	−62.5	56.4	−38.7	27.6
1 D1	39.2	−57.4	25.9	27.1	−47.2	11.3
1 E0	−44	56.4	−52.2	34.7	−22.3	27.6
1 E1	27.6	−51.8	35.7	8.6	−33.7	13.4
1 F0	−42.3	65.9	−32.1	−27.8	53	−14.8
1 F0′	−56.2	60.8	−44.1	22.1	−17.2	34.9
1 F1	20.5	−56	27.8	36.7	−74	40.4
1 F1′	−36.7	−0.7	49.5	−67.5	27.7	24.5
1 G0	−46.1	56	−57.6	50	−41.3	39.8
1 G1	−28.4	−25.6	53.7	−21	−35.5	63.4
2 B0	−10.3	48.3	−60.9	32.4	8.2	−20.2
2 B1	59.9	−62.6	36.5	−3.9	1.6	−31.7
2 C0	−40.6	51.2	−59.4	58.6	−46.8	37.4
2 C1	48.2	−59.1	55.1	−40.6	31.8	−36.4
2 D0	−40	49.7	−59.9	61	−49.8	39.3
2 D1	47.9	−57.9	53.6	−39	31.1	−36.6
2 E0	−37.5	50.9	−61.3	58.9	−43.9	33
2 E1	43.1	−52.8	51.3	−41.4	34.1	−35.1
2 F0	−61.4	54.6	−2.5	−49	42.3	13.7
2 F1	56.1	−53.2	50.4	−50.2	50.3	−54.5
2 G0	−47.2	59.3	−57.4	44.9	−33.3	34.4
2 G1	34.9	−64.5	35.4	25.1	−56.8	23.1
B0–**C0** TS1 **1**	−34.2	58.8	−55.6	29.5	−5	7.4
B0–**C0** TS2 **1**	−35.3	59.3	−52.8	22	0.5	7.1
B1–**C1** TS1 **1**	−6.7	−42.1	65.8	−37.1	−13.7	38
B1–**C1** TS1 **1**	4	−531	68.6	−29.3	−21.5	35.9
B0–**C0** TS **2**	−47	58.7	−42	13.3	−1.9	19.6
B1–**C1** TS **2**	62	−61.8	34	−3.3	4.2	−33.3
E0 Gly TS **1**	−12.6	50.5	−39.4	−13.6	55.2	−40.6
E1 Gly TS **2**	−22.2	−21.6	53.9	−39.5	−8.9	41

28 kJ mol^{-1} correction for H-bonds, see Table 1. This result compels the need for a more sophisticated model that at least includes some of the interconversion barriers like the ones between **B** and **C** species discussed above.

Our first test was to see if the **B** to **C** interconversions could be modeled by simple C-2–O-2 bond rotations. Thus, this torsion angle (CH-2-C-2–O-2-C-7) was varied in 10° increments with full geometry optimization a every point. After further optimization and characterization, the TSs for such rotations were found (see Section 2). As shown in Figure 4a–d one or two TSs were found for each case. The clearest picture emerged for

Table 4. Structural characterization of the H-bonds in selected complexes

Compound	Donor	Acceptor	O–H (Å)	H···O (Å)	O···O (Å)	O–H···O (°)
1 E0	CH_3OH	O-6	0.999	1.71	2.69	166
1 E1	CH_3OH	O-6	1.003	1.68	2.676	171.9
1 F0	CH_3OH	O-6	1.202	1.209[a]	2.405	171.6
1 F0′	CH_3OH	O-7	1.202	1.205[a]	2.399	170.9
1 F1	CH_3OH	O-6	1.208	1.208[a]	2.401	167.4
1 F1′	OH-6	O-4	1.138	1.272[a]	2.404	172.3
1 G1	CH_3OH	O-4	1.175	1.247[a]	2.395	163
1 E0 TS	CH_3OH	O-6	1.21	1.205[a]	2.412	174.1
2 E1	CH_3OH	O-4	0.996	1.693	2.668	165
2 F0	CH_3OH	O-6	1.202	1.213[a]	2.4	167.4
2 F1	OH-6	O-1	1.236	1.171[a]	2.391	167
2 G1	CH_3OH	O-4	1.167	1.261[a]	2.4	162.5
2 E1 TS	CH_3OH	O-4	1.026	1.547	2.54	161.2

[a] Short H-bonds have considerable covalent bond character.[33]

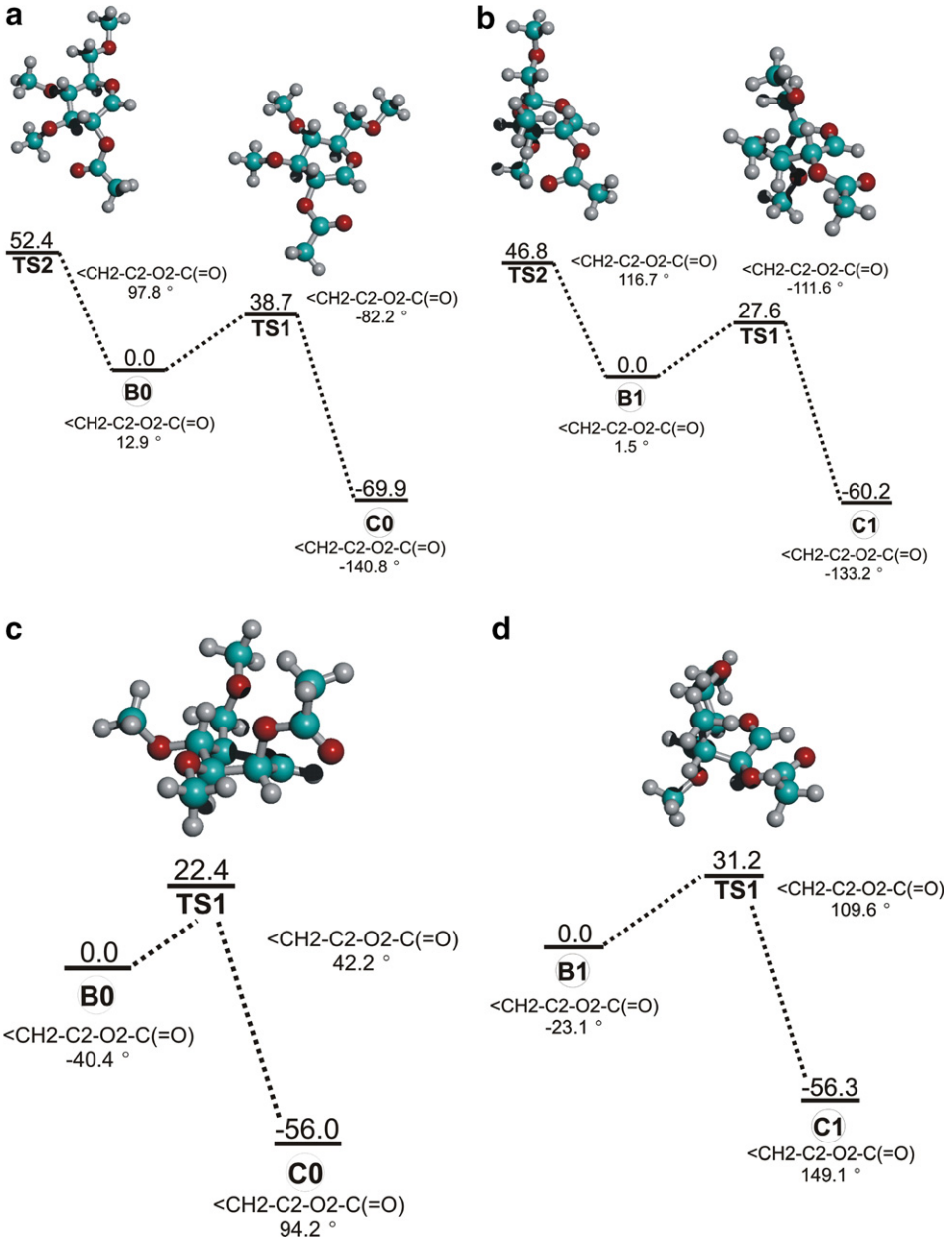

Figure 4. Possible TSs for dioxolenium ion formation (a) **B0** to **C0 1**, (b) **B1** to **C1 1**, (c) **B0** to **C0 2**, and (d) **B1** to **C1 2**.

1 where rotation toward or away from C-1 led to two TSs for both **B0** to **C0** and **B1** to **C1** conversions with values of this torsion angle near ±90°. These TSs have the ester carbonyl nearly perpendicular to a plane defined by CH-2, C-2, and O-2. This is the 'normal' barrier to C-2–O-2 bond rotation for the O-2 methyl-substituted glycopyranosyl oxacarbenium ions.[27] This barrier arises in part because of hyperconjugative interactions between the O-2 lone pairs and the C–C and the C–H bonds attached to C-2, as well as longer range interactions with the C-1 and O-5 atoms.[27] Consequently, it is anticipated that both the steric and electronic properties of the O-2 protecting group can modify this barrier (see below). The case for **2** was very similar except that the **B0** to **C0** barrier was shifted from 90° to 42.2°. The barriers are all similar to the 34 kJ mol^{-1} found for the **B0** to **C1** transformation of **3**, although the origin of the barrier is very different. Examination of the canonical vector coefficients describing the ring conformations of all these **B** to **C** TSs clearly shows that the ring conformations change only slightly (Table 2). The determination of **B0** to **C1** and related transformation involving ring inversion have not been investigated yet for **1** and **2**. These studies must be done to arrive at a firm conclusion, but tentatively it appears that **3** is anomalous, perhaps consistent with its tendencies for related glycosyl donors to give acyl-transfer side reactions.

The recognition that species like **D** should play a role in neighboring-group assisted glycosylations has been recognized for a number of years.[28] However, the mechanism by which the **D** species lead to glycosides is largely unknown, although several suggestions have been put forth.[29] Many of these suggestions relate to the mechanism of orthoester glycosylation. Most orthoester glycosylations rearrange neutral orthoesters with protic acid or strong Lewis acids. Several experimental facts are pertinent to this discussion including that if two different orthoesters are rearranged in the same pot, the alcohol portions are fully exchanged, strongly supporting an intermolecular mechanism based on protonation, disassociation, recombination at C-1 and deprotonation.[30] The order of C-1 recombination and deprotonation cannot be deduced from these results. These observations obviously support the formation of species like **D** on the route to neutral glycosides from neutral orthoesters, recognizing that Lewis acids can be exchanged for protons, although the detailed mechanisms are clearly different.[31] We have computationally examined many of these plausible pathways, but none of our results have satisfactorily explained glycosylation. Importantly, we have never found a five-coordinate S_N2 TS that corresponds to the one drawn in most depictions of neighboring group participation (upper right Scheme 4). Three such mechanisms are shown in Scheme 4. All our efforts have led either to species that are not TSs, that is, do not have one imaginary frequency or are of implausibly high energy. Another key result from our studies is that the potential energy surface (PES) separating the **D** species from the **E** species is so shallow that they should interconvert rapidly, that is, the first step of mechanism 1 in Scheme 4 appears feasible, but not the 2nd.

These failures have led us to consider other possibilities. For example, based on our result that proton transfer from the **D** species to O-2 is a trigger for the acyl-transfer species, we wondered if proton transfer to either O-1 or O-5 could be a trigger to glycosylation. To this end we performed the calculations shown in Scheme 5. Protonation at either O-1 or O-5 is energetically uphill and appears not to be a viable pathway. Protonation on O-2 leads to acyl transfer and is exothermic.

Next we reasoned that if C-2–O-2 bond rotation led to dioxolenium ion formation, might it not lead to glycoside formation from the four **E** species that we have already shown to be in easy equilibrium with the **D** species? In two of the four cases examined, we found TSs that have the requisite one imaginary frequency by the procedure described above for **B** to **C** conversion. Furthermore, the geometric parameters of these two TSs all seem reasonable as shown in Figure 5 for **2 E1** going toward the expected α glycoside. These include that the CH_3O–C-1 bond length is 2.08 Å, and the C-1–O-7 bond length is 2.12 Å, with the CH_3O–C-1–O-7 bond angle of 158.4°, that is, nearly symmetric and linear. The CH-2-C-2–O-2-C-7 torsion angle is 95.6° which is near the expected value of 90°, and finally the incoming

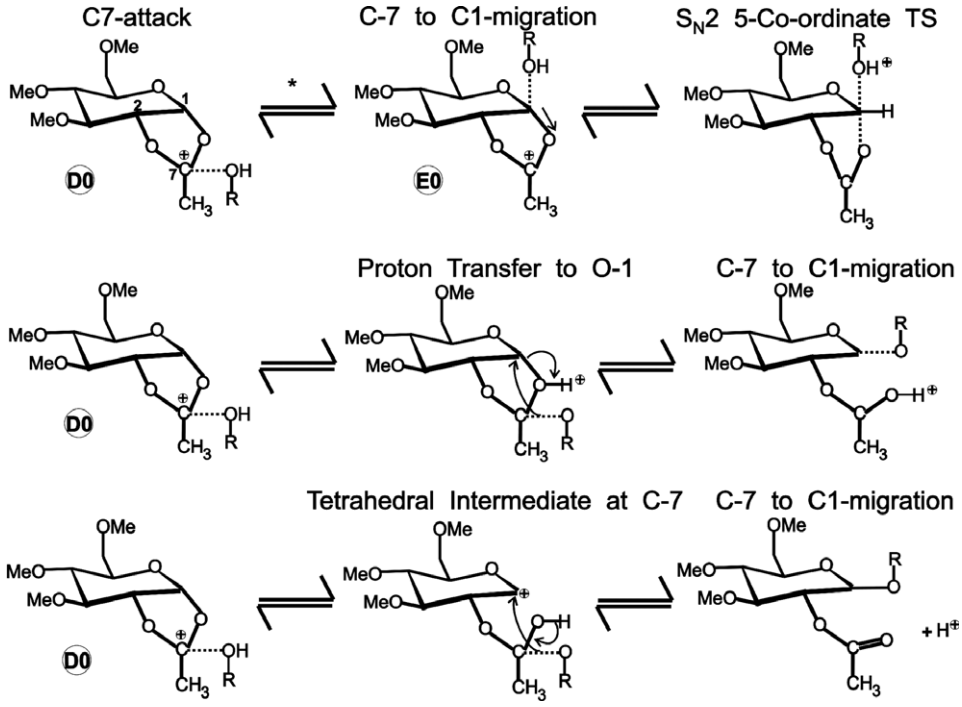

Scheme 4. Three (top, middle, and bottom) possible mechanisms for converting the **D** species to neutral glycosides following suggestions taken from the literature.

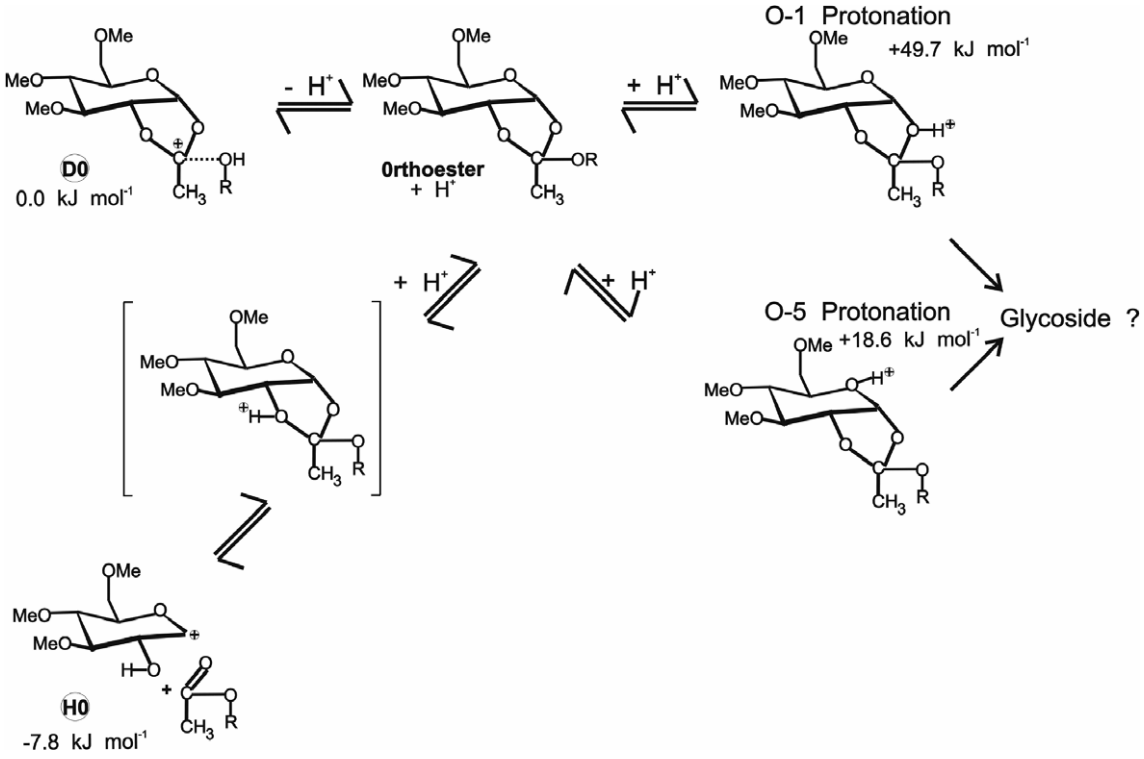

Scheme 5. Protonation of the orthoester related to **1 D0** at various oxygens. The numbers are the relative energies in kJ mol^{-1} (see Section 2).

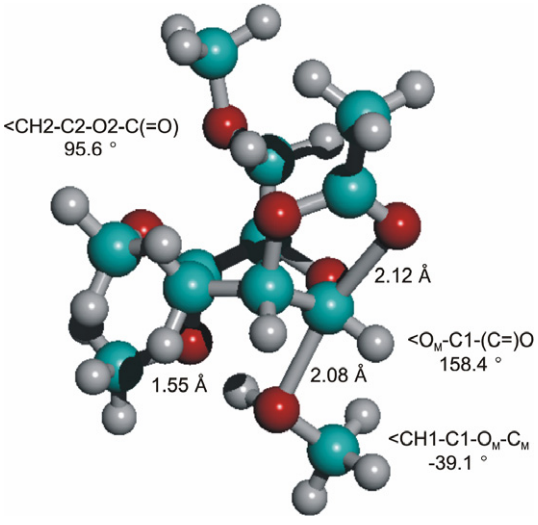

Figure 5. Ball-and-stick representation of the putative S_N2 TS for **2 E1** to the α glycoside.

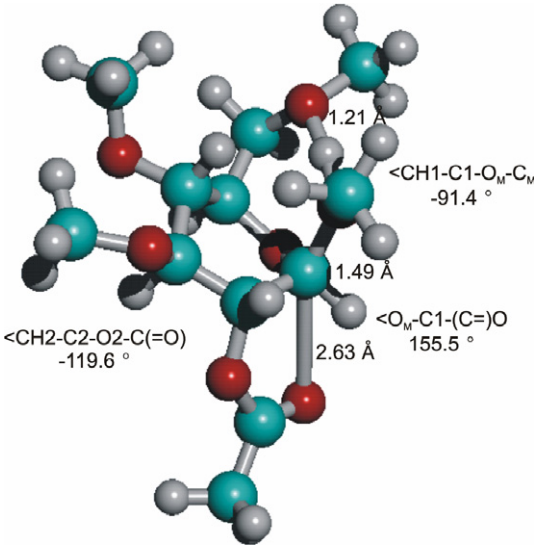

Figure 6. Ball-and-stick representation of the putative S_N2 TS for **1 E0** to β glycoside.

methanol nucleophile is approaching at a value near the −60° expected for the exo-anomeric effect, that is, the CH-1-C-1–O-CH_3 torsion angle is −39.1°. The ring geometry also approaches the equator of the conformational sphere and takes a conformation near $^5S_1$ 0.783. Skew boat and boat conformations have been associated with TSs for enzymatic glycosylation reactions.[32]

As shown in Figure 6 for **1 E0** going toward the expected β glycoside, the geometric parameters show some similarities. These include that the CH_3O–C-1 bond length is 1.49 Å, and the C-1–O-7 bond length is 2.63 Å, with the CH_3O–C-1-O-7 bond angle of 155.5°, that is, not symmetric but linear. The CH-2-C-2–O-2-C-7 torsion angle is −119.6°, which is near the expected value of −90°, and finally the incoming methanol nucleophile is approaching at a value nearer the secondary

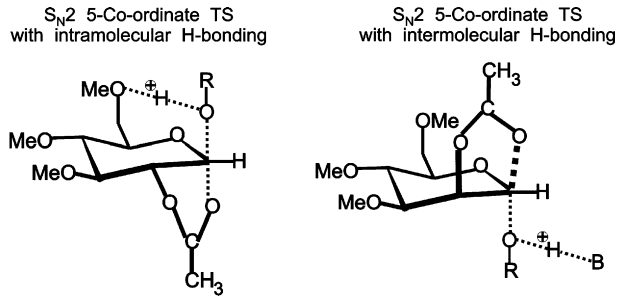

Scheme 6. Putative S_N2 TSs for the glycosylation reaction involving intra- or intermolecular H-bonds between the incoming nucleophile and suitably disposed electronegative atoms.

minimum at −60°, that is, the CH-1-C-1–O-CH_3 torsion angle is −91.4°. Finally the ring conformation is $^1S_3$ 0.882, which is also near the conformational equator. The TS starting from **2 E1** is 26.8 kJ mol^{-1} above **2 E1**, and the TS starting from **1 E0** is 12.9 kJ mol^{-1} above **1 E0**.

The key feature of these two TSs that was not recognized until now is the presence of intramolecular H-bonds. Both TSs exhibit this characteristic effect with the gluco-configured one having a very strong H-bond that is likely the origin of the distorted geometric parameters, compared to those of the manno-configured case. These results have led us to hypothesize that, in the absence of a suitable intramolecular H-bond acceptor, the neighboring-group participation TS will have an intermolecular H-bond as shown schematically in Scheme 6. The most likely candidate for the H-bond acceptor is the counteranion that is ion paired to the oxacarbenium ion.

4. Conclusions

These new DFT QM calculations on **1** and **2** and some of their plausible methanol complexes have reiterated some previous tentative conclusions. These are most notably: (1) These studies provide further examples of the two conformers of glycopyranosyl oxacarbenium ion theory, that is, **B0** to **G0** versus **B1** to **G1**. (2) They provide further examples for a pseudoequatorial conformational preference for O-2 in glycopyranosyl oxacarbenium ions, including the marked stability of $^5S_1$ conformations for gluco-configured ions. (3) They also include numerous examples of glycopyranosyl oxacarbenium ions that have nonplanar values of the O-5–C-1 (τ5) torsion angle. These conformations arise due to additional interactions with nucleophiles. All three of these conclusions markedly affect the numerous attempts to design TS mimics of the glycopyranosyl oxacarbenium ion TSs postulated to occur in GPEs. The first strongly suggests that such enzymes need to be classified as **B0**- or **B1**-utilizing enzymes. The second suggests that TS mimics should have the equivalent to O-2 in a pseudoequatorial disposition relative to the positively charged and/or flat portion of the mimic. The third suggests that, at least in some cases, such TSs may be nonplanar about C-1, and mimics may need to accommodate this property.

Two new insights emerged from these studies. The first relates to the possible importance of intramolecular H-bonds and the obligatory proton-transfer step in glycosylations. Although we have speculated previously on its importance,[5] its probable importance was not clearly established until the discovery of the TSs for neighboring group participation shown in Figures 5 and 6. Based on these results we speculate that the proton-transfer step is linked to the nucleophilic attack, and therefore all such glycosylations require a suitably oriented basic site to proceed. The orientations of bases can be controlled by synthetic chemists, either by the choice of protecting groups or by the addition of additives to glycosylation reactions. The second insight is that the motion of the leaving group in the S_N2 like opening of neighboring group **E** ions is not a bond stretching as normally depicted, but rather a CH-2-C-2–O-2-C-7 bond rotation. This bond rotation is subject to control by choice of protecting groups at O-2. It is also affected by other protecting groups on the donor sugar, especially at O-3 since interactions of the O-2 and O-3 protecting groups can occur depending on the C-2–O-2 torsion angle above and other conformational aspects of the donor. Furthermore, this conformational preference can be studied by QM calculations, thus providing a strategy for optimizing neighboring-group glycosylation reactions.

Acknowledgments

This work was partly supported by the HPC multiscale modeling initiative of the NRC. The authors thank the NRC computer support group (IMSB) for ongoing assistance. This is NRC paper 42518.

Supplementary data

Cartesian and internal coordinates for all stationary points discussed in this paper are available as supplementary data. Supplementary data associated with this article can be found, in the online version, at doi:10.1016/j.carres.2007.03.030.

References

1. (a) Whitfield, D. M.; Douglas, S. P. *Glycoconjugate J.* **1996**, *13*, 5–17; (b) Paulsen, H. *Angew. Chem., Int. Ed. Engl.* **1982**, *21*, 155–175; (c) Demchenko, A. V. *Curr. Org.*

Chem. **2003**, *7*, 35–79; (d) Kochetkov, N. E. In *Studies in Natural Products Chemistry*; Rahman, A., Ed., 1994; Vol. 14, pp 201–266.
2. (a) Suzuki, S.; Matsumoto, K.; Kawamura, K.; Suga, S.; Yoshida, J.-I. *Org. Lett.* **2004**, *6*, 3755–3758; (b) Boebel, T. A.; Gin, D. Y. *J. Org. Chem.* **2005**, *70*, 5818–5826; (c) Denekamp, C.; Sandlers, Y. *J. Mass Spectrom.* **2005**, *40*, 1055–1063; (d) Crich, D.; Chandrasekera, N. S. *Angew. Chem., Int. Ed.* **2004**, *43*, 5886–5889.
3. (a) Smith, D. M.; Woerpel, K. A. *Org. Biomol. Chem.* **2006**, *4*, 1195–1201; (b) Lucero, C. G.; Woerpel, K. A. *J. Org. Chem.* **2006**, *71*, 2641–2647.
4. (a) Ionescu, A. R.; Whitfield, D. M.; Zgierski, M. Z.; Nukada, T. *Carbohydr. Res.* **2006**, *341*, 2912–2920; (b) Nukada, T.; Bérces, A.; Wang, L. J.; Zgierski, M. Z.; Whitfield, D. M. *Carbohydr. Res.* **2005**, *340*, 841–852.
5. For our previous studies in this area see: (a) Whitfield, D. M.; Douglas, S. P.; Tang, T. H.; Csizmadia, I. G.; Pang, H. Y. S.; Moolten, F. L.; Krepinsky, J. J. *Can. J. Chem.* **1994**, *72*, 2225–2238; (b) Nukada, T.; Bérces, A.; Zgierski, M. Z.; Whitfield, D. M. *J. Am. Chem. Soc.* **1998**, *120*, 13291–13295; (c) Nukada, T.; Bérces, A.; Whitfield, D. M. *J. Org. Chem.* **1999**, *64*, 9030–9045; (d) Nukada, T.; Bérces, A.; Whitfield, D. M. *Carbohydr. Res.* **2002**, *337*, 765–774; (e) Bérces, A.; Whitfield, D. M.; Nukada, T.; do Santos, Z. I.; Obuchowska, A.; Krepinsky, J. J. *Can. J. Chem.* **2004**, *82*, 1157–1171; (f) Nukada, T.; Whitfield, D. M. *ACS Symp. Ser.* **2006**, *932*, 265–300.
6. For example: (a) Winstein, S.; Buckles, R. E. *J. Am. Chem. Soc.* **1942**, *64*, 2780–2801; (b) Frush, H. L.; Isbell, H. S. *J. Natl. Bur. Stand.* **1941**, *27*, 413–428; (c) Garegg, P. J.; Kvarnström, I. *Acta Chem. Scand.* **1977**, *B31*, 509; (d) Tichý, M.; Pánková, M. *Coll. Czech. Chem. Commun.* **1975**, *40*, 647–657; (e) Crich, D.; Dai, Z.; Gastaldi, S. *J. Org. Chem.* **1999**, *64*, 5224–5229.
7. (a) Lemieux, R. U. *Can. J. Chem.* **1951**, *29*, 1079–1091; (b) Lemieux, R. U. *Adv. Carbohydr. Chem.* **1954**, *9*, 1–57.
8. (a) Zeng, Y.; Ning, J.; Kong, F. *Tetrahedron Lett.* **2002**, *43*, 3729–3732; (b) Yang, F.; He, H.; Du, Y.; Lü, M. *Carbohydr. Res.* **2002**, *337*, 1165–1169; (c) Zeng, Y.; Ning, J.; Kong, F. *Carbohydr. Res.* **2003**, *338*, 307–311; (d) Imamura, A.; Ando, H.; Korogi, S.; Tanabe, G.; Muraoka, O.; Ishida, H.; Kiso, M. *Tetrahedron Lett.* **2003**, *44*, 6725–6728; (e) Ikeda, T.; Yamauchi, K.; Nakano, D.; Nakanishi, K.; Miyashita, H.; Ito, S.-I.; Nohara, T. *Tetrahedron Lett.* **2006**, *47*, 4355–4359.
9. Bérces, A.; Nukada, T.; Whitfield, D. M. *J. Am. Chem. Soc.* **2001**, *123*, 5460–5464.
10. Ionescu, A.; Wang, L.-J.; Zgierski, M. Z.; Nukada, T.; Whitfield, D. M. *ACS Symp. Ser.* **2006**, *930*, 302–319.
11. (a) Banoub, J.; Bundle, D. R. *Can. J. Chem.* **1979**, *57*, 2091–2097; (b) Magnus, V.; Vikić-Topić, D.; Iskrić, S.; Kveder, S. *Carbohydr. Res.* **1983**, *114*, 209–224.
12. (a) Wulff, G.; Röhle, G. *Angew. Chem., Int. Ed. Engl.* **1974**, *13*, 157–170; (b) Braccini, I.; Derouet, C.; Esnault, J.; du Penhoat, C. H.; Mallet, J.-M.; Michon, V.; Sinaÿ, P. *Carbohydr. Res.* **1993**, *246*, 23–41; (c) Crich, D. *J. Carbohydr. Chem.* **2002**, *21*, 667–690.
13. (a) Baerends, E. J.; Ellis, D. E.; Ros, P. *Chem. Phys.* **1973**, *2*, 41–51; (b) te Velde, G.; Baerends, E. J. *J. Comput. Phys.* **1992**, *99*, 84–98; (c) Fonseca Guerra, C.; Snijders, J. G.; te Velde, G.; Baerends, E. J. *Theor. Chim. Acta* **1998**, *99*, 391–403; (d) Versiuis, L.; Ziegler, T. *J. Chem. Phys.* **1988**, *88*, 322–328; (e) Fan, L.; Ziegler, T. *J. Chem. Phys.* **1992**, *96*, 9005–9012.
14. Vosko, S. H.; Wilk, L.; Nusair, M. *Can. J. Phys.* **1980**, *58*, 1200–1211.
15. Becke, A. D. *Phys. Rev. A* **1988**, *38*, 3098–3100.
16. Perdew, J. P. *Phys. Rev. B* **1986**, *34*, 7506–7516.
17. Bérces, A.; Nukada, T.; Whitfield, D. M. *Tetrahedron* **2001**, *57*, 477–491.
18. Asano, N. *Glycobiology* **2003**, *13*, 93R–104R.
19. da Silva, C. O. *Theor. Chem. Acc.* **2006**, *116*, 137–147.
20. (a) Lucero, C. G.; Woerpel, K. A. *J. Org. Chem.* **2005**, *71*, 2641–2647; (b) Shenoy, S. R.; Smith, D. M.; Woerpel, K. A. *J. Am. Chem. Soc.* **2006**, *128*, 8671–8677.
21. Stubbs, J. M.; Marx, D. *Chem. Eur. J.* **2005**, *11*, 2651–2659.
22. Berti, P. J.; McCann, J. A. B. *Chem. Rev.* **2006**, *106*, 506–555.
23. (a) Houdier, S.; Vottero, P. J. A. *Carbohydr. Res.* **1992**, *232*, 349–352; (b) Tokimoto, H.; Fujimoto, Y.; Fukase, K.; Kusumoto, S. *Tetrahedron: Asymmetry* **2005**, *16*, 441–447.
24. Fréchet, J. M.; Schuerch, C. *J. Am. Chem. Soc.* **1972**, *94*, 604–609.
25. Crich, D.; Vinogradova, O. *J. Org. Chem.* **2006**, *71*, 8473–8480.
26. (a) Mazurek, M.; Perlin, A. S. *Can. J. Chem.* **1965**, *43*, 1918–1923; (b) Fraser-Reid, B.; Grimme, S.; Piacenza, M.; Mach, M.; Schlueter, U. *Chem. Eur. J.* **2003**, *9*, 4687–4692.
27. Ionescu, A. R.; Whitfield, D. M.; Zgierski, M. Z., unpublished observations, see also Ref. 10.
28. (a) Garreg, P. J.; Norberg, T. *Acta Chem. Scand. B* **1979**, *33*, 116–118; (b) Wulff, G.; Röhle, G. *Angew. Chem., Int. Ed. Engl.* **1974**, *13*, 157–216.
29. Kong, F. *Carbohydr. Res.* **2007**, *342*, 345–373.
30. Yang, Y.; Lin, W.; Yu, B. *Carbohydr. Res.* **2000**, *329*, 879–884.
31. (a) Bochkov, A. F.; Betaneli, V. I.; Kochetkov, N. K. *Bioorg. Khim.* **1977**, *3*, 39–45; (b) Bochkov, A. F.; Betaneli, V. I.; Kochetkov, N. K. *Bioorg. Khim.* **1976**, *2*, 927–941.
32. For example, see: Money, V. A.; Smith, N. L.; Scaffidi, A.; Stick, R. V.; Gilbert, H. J.; Davies, G. J. *Angew. Chem., Int. Ed.* **2006**, *45*, 5136–5140.
33. Jeffrey, G. A.; Sanger, W. In *Hydrogen Bonding in Biological Structures*; Springer: Berlin, 1991.